



Reproducibility of Three-Dimensional Volumetric Measurement of Periorcular Tumor Models

Wanlin Fan · Alexander C. Rokohl · Patrick Kupka ·
Xiaoyi Hou · Jinhua Liu · Senmao Li · Adam Kopecky ·
Sitong Ju · Philomena A. Wawer Matos · Yongwei Guo ·
Ludwig M. Heindl

Received: August 22, 2022 / Accepted: October 6, 2022 / Published online: October 16, 2022
© The Author(s) 2022

ABSTRACT

Introduction: In this study, we measured the volume of customized tumor models in the periorcular area using three-dimensional (3D) stereophotogrammetry and evaluated the reproducibility of these measurements.

Methods: Five tumor models of different colors and sizes were placed in different periorcular

positions, and 3D facial images were obtained from 68 healthy adult volunteers. Subsequently, the volumes of the tumor models were measured, and the intra- and interrater reproducibility was assessed.

Results: The gray 6 mm model revealed the highest reliable measurements in both Caucasians (intra- and interrater intraclass correlation coefficients of 0.981 and 0.899, mean absolute difference of 1.446 and 3.327 mm³, relative error measurement of 3.497% and 8.120%, technical error of measurement of 1.450 and 3.105 mm³, and relative technical error of measurement of 3.506% and 7.580%) and Asians (0.968 and 0.844, 1.974 and 4.067 mm³, 4.772% and 9.526%, 2.100 and 4.302 mm³, and 5.076% and 10.076%, respectively). The highest reliability of measurements in the lateral upper eyelid (0.88 and 0.95, 4.042 and 3.626 mm³, 9.730% and 9.020%, 5.714 and 3.358 mm³, and 9.730% and 8.350%, respectively) and medial upper eyelid (0.81 and 0.89, 4.313 and 4.226 mm³, 9.730% and 9.020%, 6.098 and 4.069 mm³, and 9.730% and 8.350%, respectively) with eyes closed was evident in Caucasians, while the same trend (0.841 and 0.815, 2.828 and 3.757 mm³, 9.860% and 9.840%, 4.052 and 4.308 mm³, and 9.860% and 9.740%, respectively) was observed in Asians in the medial canthus with eyes closed.

Conclusions: This study confirms, for the first time, the high reliability of periorcular tumor volume measurements using 3D

Yongwei Guo and Ludwig M. Heindl have contributed equally to this work and share senior authorship.

W. Fan · A. C. Rokohl · P. Kupka · X. Hou · J. Liu ·
S. Li · S. Ju · P. A. W. Matos · L. M. Heindl (✉)
Department of Ophthalmology, Faculty of Medicine
and University Hospital Cologne, University of
Cologne, Kerpener Strasse 62, 50937 Cologne,
Germany
e-mail: ludwig.heindl@uk-koeln.de

A. C. Rokohl · L. M. Heindl
Center for Integrated Oncology (CIO), Aachen-
Bonn-Cologne-Dusseldorf, Cologne, Germany

A. Kopecky
Ophthalmology Clinic, University Hospital Ostrava,
Ostrava, Czech Republic

Y. Guo (✉)
Eye Center, Second Affiliated Hospital, Zhejiang
University School of Medicine, 88 Jiefang Road,
Hangzhou 310009, China
e-mail: yongwei-guo@zju.edu.cn

Y. Guo
Zhejiang Provincial Key Lab of Ophthalmology,
Hangzhou, China

stereophotogrammetry, suggesting its feasibility for eyelid tumor measurement. Further trials are required to investigate its clinical use for documentation and follow-up of different eyelid tumors.

Keywords: Reproducibility; Stereophotogrammetry; Three-dimensional; Tumor; Volume

Key Summary Points

Three-dimensional imaging systems have questionable reliability for volume measurements in the periocular region.

We aimed to evaluate the reliability of the Vectra M3 3D imaging system for periocular volume measurement.

This study confirms the high reliability of volume measurement of larger gray tumor models, especially in the medial canthus of the closed eye in Asians.

Further trials are required to investigate its clinical use for documentation and follow-up of different eyelid tumors.

INTRODUCTION

The periocular region consists of the upper and lower eyelids, medial canthus, lacrimal system, and lateral canthus. Owing to increased exposure to ultraviolet (UV) radiation, the incidence of skin cancer in this anatomical location is relatively high. Approximately 5–10% of skin malignancies occur in the periocular region. Basal cell carcinoma (BCC) is the most common periocular malignancy, followed by squamous cell carcinoma (SCC), sebaceous gland carcinoma (SGC), and cutaneous melanoma [1]. Periocular tumors occur more frequently in the lower eyelid (48%) or medial canthus (27%) than in the upper eyelid (25%), which is protected from UV radiation by the eyebrows [2]. Periocular tumors may affect the function and esthetics of the eye, with potentially devastating effects on the patient's vision and quality of

life [3]. In addition, periocular tumors are adjacent to important sites such as the orbit, sinuses, and brain, and often develop and metastasize without being detected by the patient or physician [4]. Therefore, timely diagnosis and treatment of periocular tumors, especially malignant tumors, is vital. The periocular region has a relatively constricted anatomy; therefore, limited surgical excision may require reoperation, while aggressive tissue excision may require extensive tissue reconstruction. Therefore, ensuring complete removal of eyelid tumors with safe margins while preserving as much eyelid and surrounding tissues as possible is a challenge. Quantitative measurement analysis of periocular images is expected to address this issue.

Stereophotogrammetry is currently the most promising technique for soft tissue assessment. It uses a high-resolution and fast-acquisition camera system to capture images of individuals from different angles and reconstruct a three-dimensional (3D) image. A typical static 3D imaging device, Vectra M3 (Canfield Scientific, Fairfield, NJ, USA), consists of six cameras in three modules mounted on a tripod. The system has a resolution of 1.2 mm and an acquisition time of 3.5 ms, and costs more than 50,000 euros. With the development of high-resolution camera technology, 3D imaging systems have been widely used in craniofacial, maxillofacial, and facial esthetic procedures [5, 6] and are being increasingly used for ophthalmic applications and studies. In recent studies, detailed protocols for periocular landmarks have been developed [7, 8], and the accuracy and reliability of linear, angular, and area measurements in the periocular region have been verified [9–12]. However, the reproducibility of volumetric measurements in the periocular region has not been fully validated. A study has indicated that the use of 3D imaging systems to assess changes in periorbital surface volume is accurate and has interobserver reproducibility [13]. Stereoscopic volume measurements with 3D imaging systems have a great potential for applications in the diagnosis of diseases of the periorbital region, treatment monitoring, and assessment of surgical outcomes (for example, assessment of eyelid tumors, scars, or lesions).

In this study, we evaluated the reproducibility of the Vectra M3 3D imaging system to measure the volume of different 3D-printed tumor models at different periocular locations, thus demonstrating the feasibility of this system for quantifying the volume of periocular tumors.

METHODS

Participant Population

On the basis of a two-sided 5% significance level with 80% power and medium effect size, this study recruited 68 ethnically diverse healthy adults aged < 50 years. All participants provided written informed consent. This study followed the principles of the Declaration of Helsinki and was approved by the Ethics Committee of the University of Cologne (approval number 17-199). All of the patients gave specific consent for the publication of their data and images.

3D-Printed Models

The company, 3DPRINT.LU (AMSOL, Luxembourg) designed and printed five resin models using a 3D printer (Table 1). Flesh-colored semicircular models of diameters of 6, 4, and 2 mm were numbered 1, 2, and 3, respectively, and black and gray semicircular models of 6 mm diameter each were numbered 4 and 5, respectively. Models 1–5 were placed in the middle of the lower eyelid and underneath the eyelid margin (Fig. 1). Eight identical models numbered 1 were simultaneously affixed to eight different periocular locations: the exocanthion, endocanthion, and upper medial, upper middle, upper lateral, lower medial, lower middle, and lower lateral eyelids (Fig. 1). Each model was affixed at a distance of 5 mm from the eyelid margin to minimize the effect of eyelashes on the measurement.

3D Image Acquisition

Volunteers with eyes open and closed were photographed using the VECTRA M3 3D imaging system. Before taking the pictures, the volunteer's hair was pulled back to expose the entire face. The face should not have any makeup to obtain a clear image. Volunteers were asked to sit in front of the camera with their heads straight and facial expressions relaxed. An experienced researcher and photographer (W.F.) acquired the images under the same lighting conditions.

Data Measurements

Two independent raters [rater 1 (W.F.) and rater 2 (P.K.)] performed the measurements on a standard desktop computer using the software provided by VECTRA M3 (VECTRA 3D analysis module). Rater 1 repeated measurements twice for each image (measurements 1.1 and 1.2), and rater 2 performed the measurements only once for each image (measurement 2.1).

Volume Difference Between Two Surfaces (Parallel Projection)

The volume measurements were performed as follows: from the obtained images, pre (before adding the 3D model volume) and post (after adding the 3D model volume) surface images were selected. These two surfaces were superimposed by aligning the surface area [14] (Fig. 2A). The superimposed images were verified to be in accurate alignment in 3D to avoid registration artifacts. When two surfaces are superimposed, the volumetric analysis software produces a quantitative measure of variation or error, called the root mean square (RMS) error value [15], which is calculated as the square root of the sum of the squared deviations in all three spatial directions. In previous studies, RMS threshold values equal to or less than 0.5 mm were described as the maximum clinically acceptable level of variation [16]. Therefore, we repeated the superimpositions and checked the alignment until RMS values in this range were obtained [17, 18], thereby ensuring that the

Table 1 Intra- and interrater statistical differences in 3D volume measurements

3D models	Positions	Eye status	Caucasians		Asians	
			Intrarater	Interrater	Intrarater	Interrater
1	Exocanthion	Open eye	0.018*	0.021*	0.627	0.264
		Closed eye	0.003**	0.124	0.611	0.418
	Upper lateral eyelid	Open eye	0.123	0.975	0.895	0.894
		Closed eye	0.104	0.699	0.100	0.252
	Upper middle eyelid	Open eye	0.077	0.195	0.989	0.405
		Closed eye	0.200	0.719	0.110	0.914
	Upper medial eyelid	Open eye	0.144	0.344	0.986	0.331
		Closed eye	0.103	0.712	0.152	0.993
	Endocanthion	Open eye	0.081	0.878	0.575	0.184
		Closed eye	0.349	0.398	0.475	0.272
	Lower medial eyelid	Open eye	0.018*	0.013*	0.858	0.096
		Closed eye	0.861	0.306	0.751	0.297
	Lower middle eyelid	Open eye	0.148	0.033*	0.375	0.107
		Closed eye	0.977	0.867	0.462	0.402†
	Lower lateral eyelid	Open eye	0.087	0.004**	0.643	0.153
		Closed eye	0.046*	0.433	0.410	0.561†
2	Lower middle eyelid	Open eye	0.724†	0.007**†	0.073	0.140†
3			0.111	0.363	0.071	0.139
4			0.556	0.990	0.605	0.16
5			0.307	0.634	0.197	0.043*

The *p* values stand for differences analyzed by paired *t*-test. †Represents *p* values calculated from Wilcoxon's signed-rank test.
*Represents *p* < 0.05

images were correctly superimposed (Fig. 2B). The final volumetric measurements were recorded in milliliters (mL) and calculated as the difference between the two registered surface maps in the same area (where the 3D model was placed) on the corresponding image (Fig. 2C).

Statistical Analysis

Differences between the intra- and interrater measurements were expressed as the mean absolute difference (MAD) and relative error

measurement (REM), technical error of measurement (TEM), and relative TEM (rTEM). Intra- and interrater reliability analyses were performed by comparing measurements 1.1 and 1.2 and measurements 1.1 and 2.1, respectively.

In a previous maxillofacial study, the acceptable error threshold for MAD and TEM was set to less than two units [19]. Because the values in the periorcular region are smaller, some studies have suggested that their thresholds should be less than one unit [20, 21]. REM and rTEM were graded as < 1%, 1–3.9%, 4–6.9%,

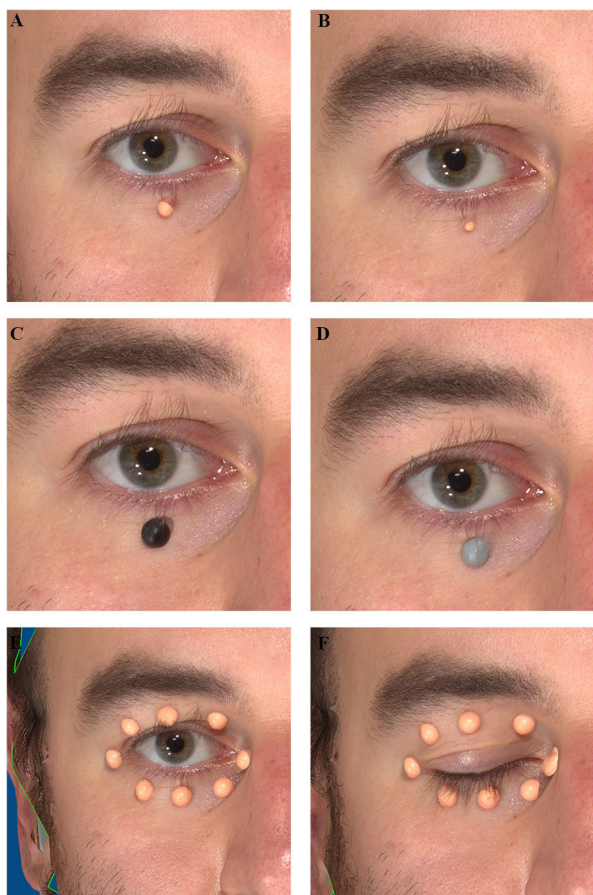


Fig. 1 3D images of the tumor model 1–5 in the periocular region. **A** Model 2 (4 mm, flesh color) in the middle of the lower eyelid; **B** model 3 (2 mm, flesh color) in the middle of the lower eyelid; **C** model 4 (6 mm, black color) in the middle of the lower eyelid; **D** model 5 (6 mm, gray color) in the middle of the lower eyelid; **E** model 1 (6 mm, gray color) in eight periocular positions—the exocanthion, the endocanthion, and the upper lateral, the upper middle, the upper medial, the lower medial, the lower middle, and the lower lateral eyelid with eyes open; **F** model 1 (6 mm, gray color) in eight periocular positions with eyes closed

7–9.9%, and > 10%, which were considered excellent, very good, good, moderate, and poor agreement, respectively [22]. The intraclass correlation coefficient (ICC) was used to assess agreement between two sets of measurements. $ICC < 0.5$ was considered poor, 0.5–0.75 was moderate, 0.75–0.9 was good, and $ICC > 0.9$ was excellent agreement [23].

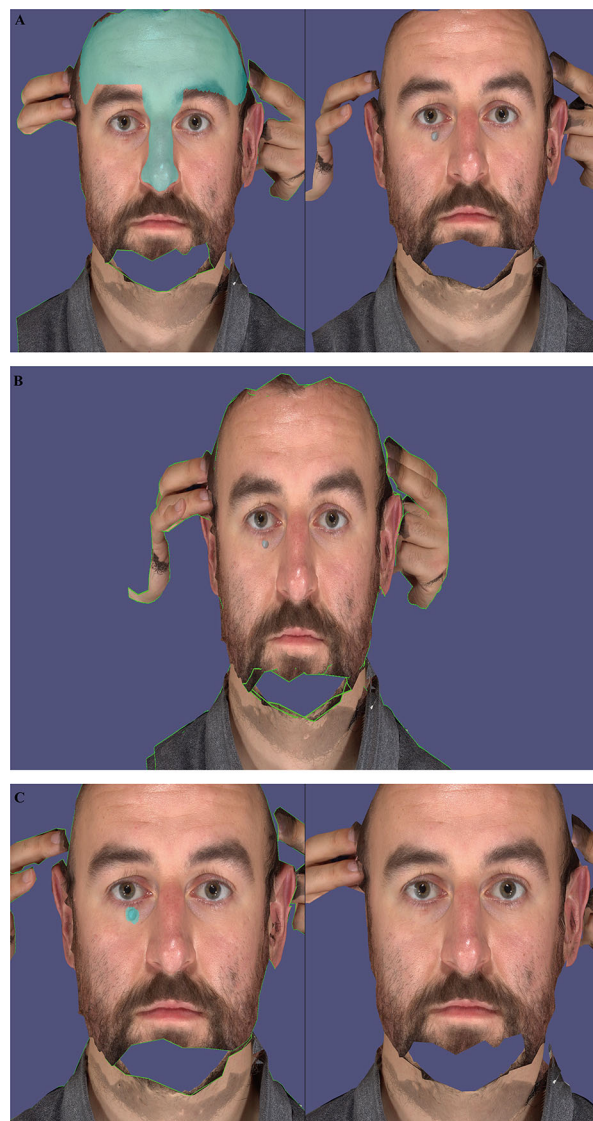


Fig. 2 Procedure for photo capture and volume measurement of periocular tumor models. Superposition and registration of two photos and measurement of volume change of periocular tumor models. **A** Superimposition of two images using surface-area-based registration; **B** images after superimposition of two photos; **C** two 3D scans with and without the tumor model were captured, and the area where the tumor model was located was selected (blue). The tumor model generates the difference between the two surfaces, and the software automatically calculates the volume

SPSS software version 26.0 (IBM, New York, NY, USA) was used for the statistical analyses. Bar charts were generated using GraphPad Prism

(GraphPad Software, Inc., San Diego, CA, USA). The Shapiro–Wilk test was used to determine whether the data were normally distributed. For normally distributed data, paired *t*-tests were applied to analyze the presence of statistically significant differences between the two data groups. The Wilcoxon signed-rank test was used for non-normally distributed data. Statistical significance was defined at $p < 0.05$.

RESULTS

Of the 68 recruited adults, 38 were female and 30 were male, aged between 19 and 44 years (mean 28.2 ± 4.0 years). Thirty-seven volunteers were of East Asian ethnicity (18 men and 19 women), and the remaining 31 volunteers were of Caucasian ethnicity (12 men and 19 women). There were no statistically significant differences in the results of paired *t*-tests or Wilcoxon signed-rank tests in Asians for all models except model 5; no statistically significant differences were found for the results at the upper eyelid and medial canthus in Caucasians (Table 1).

3D Models with Different Sizes

For Caucasians, models 1 and 2 were not significantly different in any comparison, except interrater comparison; model 3 was not significantly different in any comparison. No significant differences were found in Asian periocular measurements for any comparison. Among the three flesh-colored semicircular models [models 1 (6 mm), 2 (4 mm), and 3 (2 mm)], the reliability of measurements of the larger model 1 was relatively better in both Caucasians (good intra- and interrater ICC and moderate intrarater REM) and Asians (excellent intrarater ICC, good interrater ICC and intrarater REM, and moderate rTEM) (Fig. 3).

3D Models with Different Colors

Among Caucasians, no comparison was significantly different except interrater comparisons for model 1. In Asians, data showed no

statistically significant differences in any comparison, except interrater comparisons for model 5. Of the three larger semicircular models of different colors [models 1 (flesh color), 4 (black), and 5 (gray)], measurements of the gray model 5 had relatively better reliability in the middle lower eyelid in both Caucasians and Asians, followed by those of the flesh-colored model 1 and black model 4. For gray model 5 measurements, Caucasians exhibited intrarater MAD and TEM less than 2 mm^3 , excellent intra- and interrater ICC, very good intrarater REM and rTEM, and moderate interrater REM and rTEM; intrarater MAD in Asians was less than 2 mm^3 , and they showed excellent intrarater ICC, very good inter-rater ICC, good intrarater REM, and moderate rTEM (Fig. 3).

3D Models at Different Positions

Eyes Open

With eyes open, four periocular positions in Caucasians (lateral, middle, and medial upper eyelid and endocanthion) and all eight periocular positions in Asians were not significantly different in any comparison. The reliability of measurements in the endocanthion and upper lateral eyelid was relatively better in both Caucasians and Asians with eyes open. In the endocanthion, the intrarater MAD and TEM for Caucasians were less than 2 mm^3 , and they had excellent intrarater ICC, moderate interrater ICC, REM, and rTEM, and very good intrarater REM and rTEM, but most of the values (24/31 variables) in this position could not be measured. For Asians, both intra- and interrater MAD and TEM exceeded 2 mm^3 , and they had moderate intrarater ICC, intrarater REM, and interrater REM and rTEM and excellent interrater ICC. In the upper lateral eyelid in Caucasians, both intra- and interrater MAD and TEM greater than 2 mm^3 , excellent intrarater ICC and interrater ICC, and good intrarater REM and rTEM were observed. In Asians, intra- and interrater MAD and TEM were greater than 2 mm^3 , intrarater ICC and interrater ICC were excellent, and intrarater REM and interrater REM and rTEM were moderate. In general, with eyes open, Caucasians had the highest

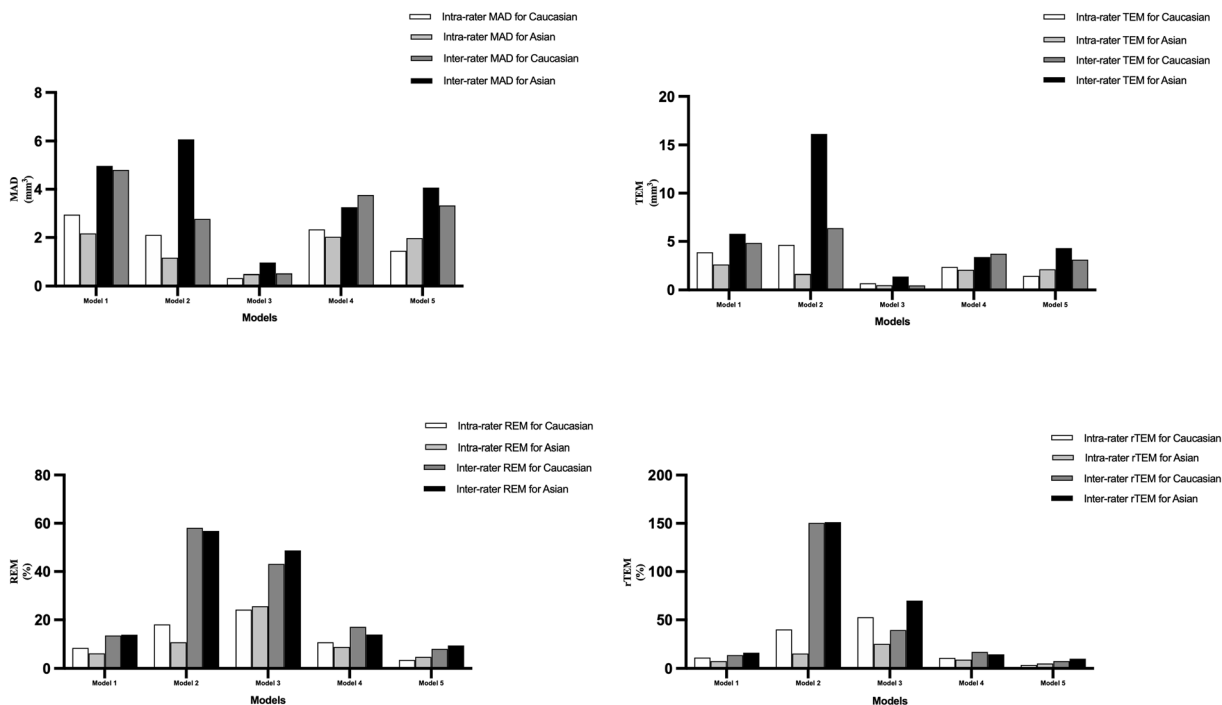


Fig. 3 Intra- and interrater reliability of MAD, TEM, REM, and rTEM for volume measurements of different tumor models. MAD mean absolute difference, TEM

technical error of measurement, REM relative error measurement (REM), rTEM relative technical error of measurement

reliability for measurements in the lateral upper eyelid, and Asians had better reliability for measurements in the medial canthus and lateral upper eyelid (Fig. 4).

Eyes Closed

With eyes closed, Caucasians exhibited no significant differences at any position except for intrarater comparisons in the endocanthion and exocanthion. Periocular volume measurements in Asians with eyes closed showed no significant differences in any position. All Caucasians had MAD and TEM greater than 2 mm³, good intrarater ICC, excellent interrater ICC, and moderate intrarater REM, interrater REM, and rTEM for the lateral upper eyelid, followed by the medial upper eyelid, for which Caucasians exhibited good intrarater and interrater ICC and moderate intrarater REM, interrater REM, and rTEM. For the medial canthus, intrarater MAD and TEM were less than 2 mm³, intrarater ICC was poor, interrater ICC and interrater REM were good, and rTEM was very

good, while both intrarater REM and rTEM were poor. At the exocanthion, MAD and TEM in all Asians were greater than 2 mm³, intrarater and interrater ICC, intrarater REM, and rTEM were good, and interrater REM and rTEM were moderate; MAD and TEM at the endocanthion were more than 2 mm³, intrarater and interrater ICC and intrarater REM were good, and intrarater rTEM, interrater REM, and rTEM were moderate. Overall, volume measurements of periocular objects were most reliable at the medial and lateral upper eyelid in Caucasians with eyes closed. Although the reliability of measurements in the medial canthus was reduced compared with that of the open eye, the results were obtained for each measurement when the eyes were closed. The reliability of measurements in the exocanthion and endocanthion was higher in Asians when the eyes were closed.

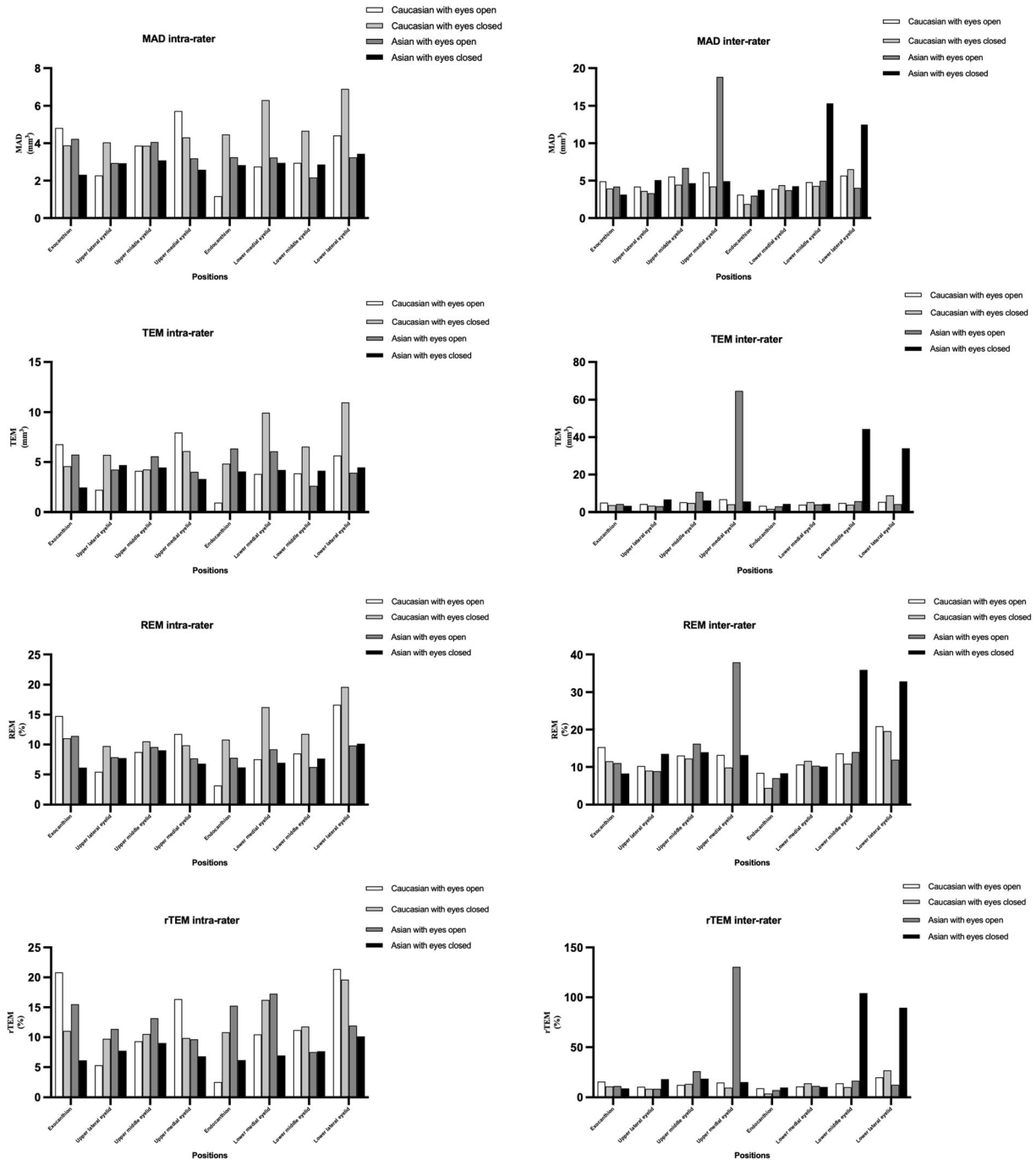


Fig. 4 Intra- and interrater reliability of MAD, TEM, REM, and rTEM for model 1 volume measurements at different periocular positions with eyes open and closed

DISCUSSION

This study creatively used an indirect measurement of the volume of a periocular tumor

model by comparing the volume changes between two parallel projected surfaces. Furthermore, this study validated the intra- and interrater reliability to assess the feasibility of

this method in clinical practice. Our findings revealed that among the five different tumor models, the largest gray model 5 (6 mm in diameter and 3 mm in height) had the highest reliability in measurement among Asians (intra- and interrater ICC: 0.968 and 0.844, MAD: 1.974 and 4.067 mm³, REM: 4.772% and 9.526%, TEM: 2.100 and 4.302 mm³, and rTEM: 5.076% and 10.076%) and Caucasians (0.981 and 0.899, 1.446 and 3.327 mm³, 3.497% and 8.120%, 1.450 and 3.105 mm³, and 3.506% and 7.580%, respectively). Of the eight different periocular locations, Caucasians had the highest reliability for measurements in the lateral upper eyelid (0.88 and 0.95, 4.042 and 3.626 mm³, 9.730% and 9.020%, 5.714 and 3.358 mm³, and 9.730% and 8.350%, respectively) and medial upper eyelid (0.81 and 0.89, 4.313 and 4.226 mm³, 9.730% and 9.020%, 6.098 and 4.069 mm³, and 9.730% and 8.350%, respectively) with eyes closed. Asians had the highest reliability for measurements in the medial canthus (0.841 and 0.815, 2.828 and 3.757 mm³, 9.860% and 9.840%, 4.052 and 4.308 mm³, and 9.860% and 9.740%, respectively) with eyes closed. This research extends the application of 3D imaging systems for volumetric measurements in the periocular region, which lays the foundation for the development of new 3D imaging techniques for the prevention, diagnosis, and postoperative evaluation of eyelid tumors.

To the best of our knowledge, this is the first study to validate 3D imaging for the assessment of periocular tumor volumes. The use of 3D imaging to assess volume changes in periorbital soft tissue and facial morphology has been reported to be reliable in several previous studies [13, 24–26]. Volume changes in the periorbital region have been accurately assessed using 3D image reconstruction with good interobserver reproducibility [13]. In addition, 3D scanning techniques are useful for assessing palatal volume in patients with cleft lip and palate [27], nasal soft tissue changes, upper lip volume after orthognathic surgery [28], breast volume [29], and volume changes in acute edema caused by burns [30].

Our study shows that the reliability of measurement of the 6-mm-diameter tumor model 1

(Caucasian: intra- and interrater ICC: 0.882 and 0.831, MAD: 2.946 and 4.804 mm³, REM: 8.520% and 13.663%, TEM: 3.871 and 4.847 mm³, and rTEM: 11.192% and 13.785%; Asian: 0.971 and 0.823, 2.167 and 4.969 mm³, 6.234% and 13.967%, 2.613 and 5.799 mm³, 7.518% and 16.301%, respectively) was higher than that of the 4-mm- and 2-mm-diameter tumor models (models 2 and 3) and showed a trend toward higher reliability with larger size. One study reported that the most common tumors in the periocular area, BCCs, are mainly 6–10 mm in diameter [31]. Furthermore, large tumor size is a risk factor for aggressive BCC [32]. Thus, our study reveals the great potential of 3D imaging devices for the volumetric measurement of large invasive eyelid BCCs.

Comparing the three different color tumor models, measurements of the gray tumor model were the most reliable, followed by those of the flesh-colored and black tumor models. The most common tumors around the eye, such as BCC and SCC, are predominantly flesh colored. In some cases, gray pigmentation can be observed in BCCs [33]. In contrast, rarer uveal melanomas are pigmented, with predominantly brown and gray pigmentations, while white and black pigmentations may also be observed [33]. Therefore, volumetric measurements of gray BCCs and eyelid melanomas using stereoscopic imaging equipment have relatively good reliability.

Periocular BCC can be found in patients of all ages, but is most common in older adults, fair-skinned individuals, and those with significant sun exposure [34]. It is reported to occur most often in the lower eyelid and inner canthus, followed by the upper eyelid and lateral canthus [34–37]. However, the incidence of BCC in the upper eyelid has been reported to be higher than that in the lower eyelid [38]. Our findings suggest that measurements of tumors in Caucasians had higher reliability in the lateral upper eyelid when the eyes are open and in the medial and lateral upper eyelids when the eyes are closed. Therefore, BCCs of the lateral upper eyelid can be considered for volumetric measurements using stereotactic imaging equipment with the eyes open. Moreover, closed eyes can improve the reliability for

measurements of BCC in the medial upper eyelid, possibly because closed eyes can reduce the interference of eyelashes on image capture and volume measurement of upper eyelid tumors. Invasion of the orbit by periocular BCC is uncommon, with a reported incidence of < 5% [39]. The most invasive BCCs in the orbit involve the medial canthus [39], and they are difficult to detect clinically because BCCs in the medial canthus rarely invade the lacrimal system through mucosal spread [40, 41]. Lesions in the lateral canthus may also present as intracranial invasion of the orbit [42]. Our results show the highest reliability in Asians for the inner and outer canthus with eyes closed, which provides a new potential approach for detection of BCC in the inner and outer canthus. SCC is common in Caucasians and Asians, with most periocular SCCs occurring in the lower eyelid, followed by the medial canthus, upper eyelid, and lateral canthus [1, 35, 43–46]. Upper eyelid SCCs in Caucasians can be considered for scanning and measurement with eyes closed, whereas measurements of upper eyelid SCCs in Asians are more reliable with eyes open and of medial and lateral canthus with eyes closed. SGCs have been reported more frequently in Asians, especially in China, India, and Nepal, with SGCs being the most common or second most common periocular malignancy in studies from these regions [47, 48]. The incidence of SGC is two to three times higher owing to the presence of more lid glands in the upper eyelid [47–49]. Therefore, for SGCs of the external upper eyelid in Asians, scanning with a 3D imaging device while the eyes are open should be considered.

This study has some limitations. First, although the reliability of volume measurements differed between groups, the overall reliability needs further improvement, which may be related to the fact that the tumor models used in this study were small and too similar in color to the skin tissue. Therefore, the reliability of the gray tumor model with a larger size needs to be investigated further. Second, because children and older adults are unable to remain stationary for long periods, we did not include them in this study to avoid introducing additional variables. Further studies are needed

to determine whether these results are consistent in children and the elderly population. In addition, we evaluated only the reliability of measuring volume changes using this method of superimposition and registration of preoperative and postoperative images and did not analyze the accuracy. Further clinical studies are required to assess the accuracy of this method. Finally, we suggest that this method should be applied clinically to assess its feasibility and treatment efficacy by measuring volume changes in patients with eyelid tumors before and after surgery. In addition, changes in tumors over time could be a sign of malignant disease; therefore, this method has a greater potential for monitoring eyelid tumors for malignant changes.

CONCLUSION

Our study confirmed the high reliability of periocular tumor volume measurements using 3D stereophotogrammetry and demonstrated the feasibility of volume measurement for eyelid tumors, particularly large gray tumors in the medial canthus. Further studies are needed to validate the 3D stereophotogrammetry technique for volumetric measurements of different eyelid tumors.

ACKNOWLEDGEMENTS

We would like to thank Editage (<http://www.editage.cn>) for English language editing.

Funding. This study was supported by the State Scholarship Fund of the China Scholarship Council (202008080258), the National Natural Science Foundation of China (82102346), and the Ministry of Health of the Czech Republic (28/RVO-FNOs/2021). The authors funded the journal's Rapid Service Fee.

Author Contributions. Conceptualization: W.F., A.R., Y.G., and L.H.; methodology: W.F. and Y.G.; formal analysis: all authors.; investigation: W.F., P.K., and A.R.; data curation: W.F.; writing-original draft preparation: W.F.;

writing-review and editing: all authors; supervision: L.H. and Y.G.; and funding acquisition: L.H. All authors have read and agreed to the published version of the manuscript.

Disclosures. Wanlin Fan, Alexander C. Rokohl, Patrick Kupka, Xiaoyi Hou, Jinhua Liu, Senmao Li, Adam Kopecky, Sitong Ju, Philomena A. Wawer Matos, Yongwei Guo, and Ludwig M. Heindl have nothing to disclose.

Compliance with Ethics Guidelines. Informed consent was obtained from all participants, and the study was carried out in accordance with the Declaration of Helsinki of 1964 and its later amendments, with approval from the Ethics Committee of the University of Cologne (approval number: 17-199). All of the patients or their guardians gave specific consent for the publication of their data and images.

Data Availability. Data from this study are available upon reasonable request to the corresponding author.

Open Access. This article is licensed under a Creative Commons Attribution-NonCommercial 4.0 International License, which permits any non-commercial use, sharing, adaptation, distribution and reproduction in any medium or format, as long as you give appropriate credit to the original author(s) and the source, provide a link to the Creative Commons licence, and indicate if changes were made. The images or other third party material in this article are included in the article's Creative Commons licence, unless indicated otherwise in a credit line to the material. If material is not included in the article's Creative Commons licence and your intended use is not permitted by statutory regulation or exceeds the permitted use, you will need to obtain permission directly from the copyright holder. To view a copy of this licence, visit <http://creativecommons.org/licenses/by-nc/4.0/>.

REFERENCES

1. Cook BE Jr, Bartley GB. Treatment options and future prospects for the management of eyelid malignancies: an evidence-based update. *Ophthalmology*. 2001;108(11):2088–98 (quiz 99–100, 121).
2. Margo CE, Waltz K. Basal cell carcinoma of the eyelid and periocular skin. *Surv Ophthalmol*. 1993;38(2):169–92.
3. Moran JM, Phelps PO. Periocular skin cancer: diagnosis and management. *Dis Mon*. 2020;66(10):101046.
4. Slutsky JB, Jones EC. Periocular cutaneous malignancies: a review of the literature. *Dermatol Surg*. 2012;38(4):552–69.
5. Day CJ, Robert T. Three-dimensional assessment of the facial soft tissue changes that occur postoperatively in orthognathic patients. *World J Orthod*. 2006;7(1):15–26.
6. Kau CH, Cronin AJ, Richmond S. A three-dimensional evaluation of postoperative swelling following orthognathic surgery at 6 months. *Plast Reconstr Surg*. 2007;119(7):2192–9.
7. Guo Y, Liu J, Ruan Y, Rokohl AC, Hou X, Li S, et al. A novel approach quantifying the periorbital morphology: a comparison of direct, 2-dimensional, and 3-dimensional technologies. *J Plast Reconstr Aesthet Surg*. 2021;74(8):1888–99.
8. Guo Y, Schaub F, Mor JM, Jia R, Koch KR, Heindl LM. A simple standardized three-dimensional anthropometry for the periocular region in a European population. *Plast Reconstr Surg*. 2020;145(3):514e–e523.
9. Guo Y, Rokohl AC, Schaub F, Hou X, Liu J, Ruan Y, et al. Reliability of periocular anthropometry using three-dimensional digital stereophotogrammetry. *Graefes Arch Clin Exp Ophthalmol*. 2019;257(11):2517–31.
10. Fan W, Guo Y, Hou X, Liu J, Li S, Ju S, et al. Validation of the portable next-generation VECTRA H2 3D imaging system for periocular anthropometry. *Front Med (Lausanne)*. 2022;9:833487.
11. Liu J, Rokohl AC, Guo Y, Li S, Hou X, Fan W, et al. Reliability of stereophotogrammetry for area measurement in the periocular region. *Aesthetic Plast Surg*. 2021;45(4):1601–10.
12. Liu J, Guo Y, Arakelyan M, Rokohl AC, Heindl LM. Accuracy of areal measurement in the periocular region using stereophotogrammetry. *J Oral Maxillofac Surg*. 2021;79(5):1106.e1–e9.

13. Hyer JN, Murta F, Juniata VAR, Ezra DG. Validating three-dimensional imaging for volumetric assessment of periorbital soft tissue. *Orbit*. 2021;40(1):9–17.
14. Wampfler JJ, Gkantidis N. Superimposition of serial 3-dimensional facial photographs to assess changes over time: a systematic review. *Am J Orthod Dentofacial Orthop*. 2022;161(2):182–97.e2.
15. Patel A, Islam SM, Murray K, Goonewardene MS. Facial asymmetry assessment in adults using three-dimensional surface imaging. *Prog Orthod*. 2015;16:36.
16. Gibelli D, Pucciarelli V, Cappella A, Dolci C, Sforza C. Are portable stereophotogrammetric devices reliable in facial imaging? a validation study of VECTRA H1 device. *J Oral Maxillofac Surg*. 2018;76(8):1772–84.
17. Naudi KB, Benramadan R, Brocklebank L, Ju X, Khambay B, Ayoub A. The virtual human face: superimposing the simultaneously captured 3D photorealistic skin surface of the face on the untextured skin image of the CBCT scan. *Int J Oral Maxillofac Surg*. 2013;42(3):393–400.
18. Jeon FHK, Griffin M, Almadori A, Varghese J, Bogan S, Younis I, et al. Measuring differential volume using the subtraction tool for three-dimensional breast volumetry: a proof of concept study. *Surg Innov*. 2020;27(6):659–68.
19. Dindaroğlu F, Kutlu P, Duran GS, Görgülü S, Aslan E. Accuracy and reliability of 3D stereophotogrammetry: a comparison to direct anthropometry and 2D photogrammetry. *Angle Orthod*. 2016;86(3):487–94.
20. Modabber A, Peters F, Kniha K, Goloborodko E, Ghassemi A, Lethaus B, et al. Evaluation of the accuracy of a mobile and a stationary system for three-dimensional facial scanning. *J Cranio-Maxillofac Surg*. 2016;44(10):1719–24.
21. Verhulst A, Hol M, Vreeken R, Becking A, Ulrich D, Maal T. Three-dimensional imaging of the face: a comparison between three different imaging modalities. *Aesthet Surg J*. 2018;38(6):579–85.
22. Ulijaszek SJ, Kerr DA. Anthropometric measurement error and the assessment of nutritional status. *Br J Nutr*. 1999;82(3):165–77.
23. Koo TK, Li MY. A guideline of selecting and reporting intraclass correlation coefficients for reliability research. *J Chiropr Med*. 2016;15(2):155–63.
24. van der Meer WJ, Dijkstra PU, Visser A, Vissink A, Ren Y. Reliability and validity of measurements of facial swelling with a stereophotogrammetry optical three-dimensional scanner. *Br J Oral Maxillofac Surg*. 2014;52(10):922–7.
25. Harrison JA, Nixon MA, Fright WR, Snape L. Use of hand-held laser scanning in the assessment of facial swelling: a preliminary study. *Br J Oral Maxillofac Surg*. 2004;42(1):8–17.
26. Hajeer MY, Mao Z, Millett DT, Ayoub AF, Siebert JP. A new three-dimensional method of assessing facial volumetric changes after orthognathic treatment. *Cleft Palate Craniofac J*. 2005;42(2):113–20.
27. Pucciarelli V, Pisoni L, De Menezes M, Ceron-Zapata AM, Lopez-Palacio AM, Codari M, et al. Palatal volume changes in unilateral cleft lip and palate paediatric patients. *Surgery*. 2015;4:6.
28. van Loon B, van Heerbeek N, Bierenbroodspot F, Verhamme L, Xi T, de Koning MJ, et al. Three-dimensional changes in nose and upper lip volume after orthognathic surgery. *Int J Oral Maxillofac Surg*. 2015;44(1):83–9.
29. Losken A, Seify H, Denson DD, Paredes AAJ, Carlson GW. Validating three-dimensional imaging of the breast. *Ann Plast Surg*. 2005;54(5):471–6.
30. Edgar D, Day R, Briffa NK, Cole J, Wood F. Volume measurement using the Polhemus FastSCAN 3D laser scanning: a novel application for burns clinical research. *J Burn Care Res*. 2008;29(6):994–1000.
31. Sin CW, Barua A, Cook A. Recurrence rates of periocular basal cell carcinoma following Mohs micrographic surgery: a retrospective study. *Int J Dermatol*. 2016;55(9):1044–7.
32. Walling HW, Fosko SW, Geraminejad PA, Whitaker DC, Arpey CJ. Aggressive basal cell carcinoma: presentation, pathogenesis, and management. *Cancer Metastasis Rev*. 2004;23(3–4):389–402.
33. Cinotti E, La Rocca A, Labeille B, Grivet D, Lambert V, Kaspi M, et al. Dermoscopy for the diagnosis of eyelid margin tumours. *Br J Dermatol*. 2019;181(2):397–8.
34. Malhotra R, Huilgol SC, Huynh NT, Selva D. The Australian Mohs database, part I: periocular basal cell carcinoma experience over 7 years. *Ophthalmology*. 2004;111(4):624–30.
35. Cook BE Jr, Bartley GB. Epidemiologic characteristics and clinical course of patients with malignant eyelid tumors in an incidence cohort in Olmsted County, Minnesota. *Ophthalmology*. 1999;106(4):746–50.
36. Carter KD, Nerad JA, Whitaker DC. Clinical factors influencing periocular surgical defects after Mohs

- micrographic surgery. *Ophthalmic Plast Reconstr Surg.* 1999;15(2):83–91.
37. Wong VA, Marshall JA, Whitehead KJ, Williamson RM, Sullivan TJ. Management of periocular basal cell carcinoma with modified en face frozen section controlled excision. *Ophthalmic Plast Reconstr Surg.* 2002;18(6):430–5.
 38. Arlette JP, Carruthers A, Threlfall WJ, Warshawski LM. Basal cell carcinoma of the periocular region. *J Cutan Med Surg.* 1998;2(4):205–8.
 39. Leibovitch I, McNab A, Sullivan T, Davis G, Selva D. Orbital invasion by periocular basal cell carcinoma. *Ophthalmology.* 2005;112(4):717–23.
 40. Fosko SW, Gibney MD, Holds JB. Basal cell carcinoma involving the lacrimal canaliculus. A documented mechanism of tumor spread. *Dermatol Surg.* 1997;23(3):203–6.
 41. Hatano Y, Terashi H, Kurata S, Asada Y, Shibuya H, Tanaka A, et al. Invasion of the lacrimal system by basal cell carcinoma. *Dermatol Surg.* 1999;25(10):823–6.
 42. Selva D, Hale L, Bouskill K, Huilgol SC. Recurrent morphoeic basal cell carcinoma at the lateral canthus with orbitocranial invasion. *Australas J Dermatol.* 2003;44(2):126–8.
 43. Malhotra R, Huilgol SC, Huynh NT, Selva D. The Australian Mohs database: periocular squamous cell carcinoma. *Ophthalmology.* 2004;111(4):617–23.
 44. Donaldson MJ, Sullivan TJ, Whitehead KJ, Williamson RM. Squamous cell carcinoma of the eyelids. *Br J Ophthalmol.* 2002;86(10):1161–5.
 45. Faustina M, Diba R, Ahmadi MA, Esmaeli B. Patterns of regional and distant metastasis in patients with eyelid and periocular squamous cell carcinoma. *Ophthalmology.* 2004;111(10):1930–2.
 46. Thosani MK, Schneck G, Jones EC. Periocular squamous cell carcinoma. *Dermatol Surg.* 2008;34(5):585–99.
 47. Nelson BR, Hamlet KR, Gillard M, Railan D, Johnson TM. Sebaceous carcinoma. *J Am Acad Dermatol.* 1995;33(1):1–15 (quiz 6–8).
 48. Song A, Carter KD, Syed NA, Song J, Nerad JA. Sebaceous cell carcinoma of the ocular adnexa: clinical presentations, histopathology, and outcomes. *Ophthalmic Plast Reconstr Surg.* 2008;24(3):194–200.
 49. Kass LG, Hornblass A. Sebaceous carcinoma of the ocular adnexa. *Surv Ophthalmol.* 1989;33(6):477–90.